



A railway track reconstruction method using robotic vision on a mobile manipulator: A proposed strategy

Miftahur Rahman, Haochen Liu ^{*}, Mohammed Masri, Isidro Durazo-Cardenas, Andrew Starr

School of Aerospace, Transport and Manufacturing, Cranfield University, Cranfield, MK43 0AL, UK



ARTICLE INFO

Keywords:
 Railway maintenance
 Sensor fusion
 3D reconstruction
 Robotic sensing
 Mobile manipulator

ABSTRACT

Autonomous robot integration in railways infrastructure maintenance accelerates the digitization and intelligence of infrastructure survey & maintenance, providing high-efficiency and low-cost execution. This paper proposes a health assessment based on 3D reconstruction technology for railway track maintenance using a mobile robotic sensing platform. By combining multiple sensing and taking advantage of a robotic manipulator, a digital model of the target track components is built by a robot-actuated vision system which provides better 3D structural and surface condition reconstruction. Global geo-location and surrounding laser scanning are integrated to reinforce the digital completeness of the model for intelligent management. The new method consists of the following steps: First, according to scheduled maintenance tasks, a Robotics Inspection and Repair System (RIRS) navigates to the task location and uses the onboard depth camera for positioning. Then robot-mounted vision system is guided with an automated trajectory to build the 3D reconstruction of the track or repair object using the vision modeling technique. Finally, the 3D reconstructed model is fused with surrounding mapping of depth vision and Lidar scanning. Both laboratory tests and a realistic track test validated the feasibility of the proposed method by creating an accurate 3D reconstructed model. The modeled rail steel section size is quantitatively compared with the ground truth in dimension, demonstrating good accuracy with a size error of less than 0.3 cm. The main contribution includes: (1) unmanned automatic 3D reconstruction by a robotic mobile manipulator, (2) the technique trims the reconstruction details & data to the specific maintenance goal or components, which supports the infrastructure maintenance towards the high-detailed & target-oriented digital management. This combination strategy of robotic automation and sensor fusion lies down a promising foundation for automated digital twin establishment for railway maintenance with autonomous RIRS, and upgrades technology readiness and digital intelligence for maintenance management

1. Introduction

As one of the crucial transportation assets, railway infrastructure networks have serviced the rise of industry and society globally for hundreds of years. The concept of asset management within a railway infrastructure environment is proposed to address the requirements of sustainable railway management from both customers and owners (Zoeteman and Esveld, 2004). Railway transportation systems include various types of infrastructures for different purposes. For example, the British railway system covers over 20,000 miles of track, 30,000 bridges, and 2500 stations, some of which are almost 200 years old, and a multitude of geographically dispersed signaling, electrification, and crossing systems (Giordano, 2018). In Europe, more than 25 billion euros cost is incurred per year to renew and maintain a 300,000 km

track and related infrastructure ("Using analytics to get European rail maintenance on track | McKinsey," n.d.). A railway infrastructure asset management system is concerned with planning, control, and maintenance of all asset-related hardware, activities, and their relationships. Railway track maintenance management is one of the basic demands to ensure safe transportation and sustainable development (Durazo-Cardenas et al., 2018). For decades, track maintenance was mostly executed by human activities, which comprised more than 40,000 people engaged in Britain to ensure the proper working condition of infrastructures (e.g., signals and power supplies) and assets (e.g., tracks and bridges) (Great Britain and Treasury, 2020).

The inspection and repair of the railway track and related jobs are crucial to the life-cycle engineering and management of track assets for ensuring the maximum usage of the railway assets. Many researchers

* Corresponding author.

E-mail address: haochen.liu@cranfield.ac.uk (H. Liu).

and international organizations are functioning together in many projects, such as Intelligent Innovative Smart Maintenance of Assets by integRated Technologies 2 (IN2SMART2), to improve the task decision support and scalable asset information management framework ("IN2SMART2," n.d.). However, due to continuous wear and asset aging, railway tracks require improved health assessment methods to ensure passenger safety and comfort. Robotic and Autonomous Systems (RAS) provide a promising and economical solution for railway maintenance (Menendez et al., 2018), which also have been proven in complex environments in other industries (Brosque and Fischer, 2022; Hu et al., 2020; Kitamura et al., 2013). Though railway track fault is a crucial reason for financial loss accounting for 17 % of train delays and 33.1 % of passenger train cancellations, only 28 % of RAS has been developed for track maintenance (R. Vithanage et al., 2019). RAS is highly demanded by combining flexibility with autonomous sensing, control, decision-making, remote communication, and work execution for inspection and repair.

With the continuous growth of railway mileage and requirements of intelligent digital infrastructure management, efficient track inspection and survey are crucial and highly demanded. Traditional vision-based track inspection methods use 2D imagery for railway infrastructure inspection or monitoring, which provides fast and high-resolution inspection for specific track fasteners (Feng et al., 2014; Gibert et al., 2015), rail-head (Li and Ren, 2012) or a tunnel (David Jenkins et al., 2017). However, these methods were designed for a single specific track component or fault by capturing without depth information with fixed-angle cameras. Laser scanning or Lidar is another option with depth sensing that can provide structural measuring and reconstruction. The generated point cloud projection can cover different structural surfaces and represents deformation and geometry amorphously. Stein et al. (Stein et al., 2016) used template matching and spatial clustering to process the laser scanning data of the railway and obtained the rail detection results through quantitative and qualitative experiments. Furthermore, a retrofitted industrial manipulator can detect and localize small components using specially designed end-of-arm tooling using multiple vision sensors and force sensors (Randika K. W. Vithanage et al., 2019). On the other hand (Zhou et al., 2017), report a railway tunnel inspection system with vehicle-based laser scanning that generates good quality mapping of tunnel internal wall. However, laser scanning cannot capture the detailed data like surface condition for small fault or defect and its point-cloud resolution is always mediocre within sensing distance. And traditional fixed laser scanner can hardly cover the whole 3D surfaces of a complex object. For example, it is difficult to cover the side and foot surfaces of the rail steel with a single scanner mounter on the train bottom. Therefore, a 3D reconstruction technique capturing high-resolution data that can manage complex shape of the track components is limited and drawing high attention.

The digital twin is a centralized and visual asset management system that can enhance operational efficiency by consolidating various information in the digital model. But due to the long mileage of the vast railway network, the substantial digital data brings computation and implementation challenges to digital twin maintenance (Wu et al., 2022). Nowadays, intelligent maintenance management is establishing the digital twin database with a smart strategy (Pan et al., 2021), which leans the high density and resolution digital model to the target components and area, rather than building or updating homogeneous details for all areas. This requires the modeling execution to have high interaction with the maintenance plans, which establish a target-oriented data-rich digital twin. The current systems normally use patrolling scanning mode and the same resolution to survey and model the whole rail network.

It will be a valuable improvement for condition monitor analysis and data efficiency of digital twin if the system can focus on the fault target area and build site-condition-based high-detailed 3D reconstruction. The relation of the fault with its 3D structure condition anomaly will support effective repair execution and condition monitoring decision-

making (Insa-Iglesias et al., 2021). A data-rich maintenance digital asset (Pastucha et al., 2020), consisting of 3D reconstruction of the target object embedded with structural dimension, condition, and its surrounding information, would definitely improve the information source and accuracy of condition monitoring for rail track components. Moreover, superimposing the 3D model over the existing map can create an Augmented Reality (AR) model, which can help the human operator to perform inspection tasks and create an intuitive plan to carry out repair tasks (Marino et al., 2021). Hence, by fusing with global-scale geo-location, middle-scale environmental laser scanning, and local-scale target reconstruction, the 3D reconstruction model will be promising to be fused with the current railway survey database to improve railway maintenance digital twin.

Hence, to achieve the above-mentioned demands, by developing an autonomous mobile manipulation platform combined with a track vehicle and an industrial manipulator, we proposed a site-condition-based 3D reconstruction technique for railway track components, which can capture the high-detailed structural and textural models using multiple remote vision sensor fusion and automated mobile manipulation.

This paper is organized as follows: several maintenance robotic cases and the robotic system in this research are stated in Section II. Section III presents the methodology and technique principles. Both a lab test and a realistic track experiment are described in Section IV to validate the proposed technique. Then the performance is discussed in Section V, which is followed by conclusions in Section VI.

2. Related research

Robots can perform many dull and mundane tasks, such as waste collection or cleaning (James et al., 2016), or can perform defect detection tasks (Chittal et al., 2017). Mobile manipulators have the potential to perform various inspection and repair tasks (Rowshandel, 2014), such as undercarriage inspection (Chiaradia et al., 2021), and rail weld bead grinding (Wu et al., 2018). Taking advantage of computer vision and deep learning, a multi-robot system has been proposed for finding various track defects (Iyer et al., 2021). Industrial robots with RGB and RGB-D cameras are capable of generating a 3D point cloud and can be used for rolling stock inspection and maintenance (R.K.W. Vithanage et al., 2019).

3D models of the target object can provide more information that can replace the current Non-Destructive Testing (NDT) methods. For example, a 3D model of a sub-millimeter pipe can be created using an existing miniature video scope camera and Structure-from-motion (SfM) technique (Dayi Zhang et al., 2022). In many cases, 3D scanning can provide better results, such as industrial parts inspection in a noisy environment (da Silva Santos et al., 2023; Zivid, n.d. *Zivid Two industrial 3D*). Similarly, 3D models of multiple railway bridges were created using three different optical digital modeling methods, and it was concluded that the 3D reconstruction method using a camera provides more portability and cost-benefit than laser scanning and infrared scanning (Popescu et al., 2019). Additionally, a 3D model of the railway track can improve rail inspection techniques (Ye et al., 2019; Dongyu Zhang et al., 2022).

A cost-benefit analysis of railway tunnels showed that data acquisition is one of the bottlenecks for 3D reconstruction techniques (Panella et al., 2020). Using robots to gather data for 3D reconstruction can improve the efficiency of data acquisition for SfM. A single fixed camera on a robot can provide imaging information in a fixed field-of-view (Reyes-Acosta et al., 2019), while an array of a camera can provide multiple images from different field-of-view (Dongyu Zhang et al., 2022). Though the latter retains better information for final output, the array of cameras requires a separate transportation system. A mobile manipulator equipped with a camera can acquire data autonomously from multiple field-of-view to reduce human involvement in the inspection method using 3D reconstruction.

A Robotic Inspection and Repair System (RIRS), shown in Fig. 1., has been proposed to reduce human involvement in the inspection and repair of the railway (Rahman et al., 2021a, 2021b). It is a mobile manipulator consisting of an Unmanned Ground Vehicle (UGV) named Warthog from Clearpath Robotics and a UR10e 6-joint manipulator from Universal Robots. The concept of RIRS is that it can be navigated both on-track and off-track with flexible inspection and repair capability powered by an industrial manipulator (Rahimi et al., 2021). Its road and rail compatibility is a unique characteristic that enables RIRS to intersect smartly with the track network according to the job location. It is more versatile than some only track-based robotic inspection and repair solutions, such as AutoScan (“AutoScan – Rail inspection by autonomous systems,” n.d.), and Railpod (“Our Platform – RailPod, Inc.,” n.d.).

To smartly perceive itself and the environment, RIRS is equipped with multiple sensors such as a Global Navigation Satellite System (GNSS) module, a 360-degree Pan-Tilt-Zoom (PTZ) environmental camera, a 3D Lidar, an RGB-D camera, and an arm-mounted RGB camera. These sensors are integrated to localize itself globally and locally, monitor the surrounding environment, find the defect characteristics, and estimate requirements for repair. Moreover, wheel encoders and an Inertial Measurement Unit (IMU) are also embedded to provide vehicle odometry and motion sensing. The RIRS is developed with an overall command and control system to power itself to autonomously navigate and execute railway infrastructure inspection and repair following the infrastructure management jobs list (Rahimi et al., 2021).

3. Methodologies

3.1. Overall methodology

Taking advantage of a RGB camera and a RGB-D camera, the RIRS can autonomously achieve inspection and site-condition-based modeling for rail components or foreign objects, supporting further repair manipulation (grind, cut, weld, or remove, etc.). In this technology, the RIRS system employs two types of cameras and a robot manipulator for visual 3D modeling: one RGB-D camera fixed in the front of the Warthog and one RGB camera attached at the end of the manipulator.

The proposed method utilizes the RIRS sensing and payload system capabilities. Fig. 2 illustrates the sequence of steps followed. By following a scheduled maintenance job, the RIRS first autonomously navigates to the job location. RIRS stops navigation once the RGB-D camera detects the target object. Then by starting the modeling process, the RGB-D camera scans and evaluates the pose of maintenance targets to the robot. The measured target pose will then be used as a concentration center to generate a reconstruction trajectory for the payload robot arm. Afterward, the RIRS guides the manipulator to model the track component target by performing automated arm manipulation with a 3D scene reconstruction scheme. With the help of



Fig. 1. The RIRS in Railway Innovation and Test Area (RITA).

the arm-tip RGB camera, images with visible information (dimension, volume, color, surface condition) of the target will be acquired for 3D reconstruction. Then, to acquire an accurate model size, a scaling process is performed by referencing a site-measured dimension of the track gauge and sleeper. Finally, the 3D reconstruction is fused with target-surrounding sensing of the vehicle depth camera, 3D Lidar, and geolocation to acquire more digital twin information and compatibility to fuse with the current infrastructure database. In the case of objects with standard measurements, such as rail or rail sleeper, volumetric information and weight of the target object can be measured by analyzing the dimensions of the reconstructed 3D model. After scaling correction, the output reconstructed model is fused with the point cloud data. Furthermore, with proper solid filling and prior standard rail material information, it is feasible to estimate the volume and mass of the target. Moreover, a reconstructed 3D model generated using images from a high-resolution RGB camera can provide the color and surface condition of the target object.

3.2. Structural model generation

A 3D structural reconstruction is a tool in computer vision that recovers the shape and appearance of an object (Liu et al., 2017; Szeliski, n.d.; “Reconstructing Rome,” n.d.). It can be done in two methods: active and passive. In the active method, sensors such as laser, ultrasound, or microwave interact with the object actively and create a 3D profile. The passive method is based on images from a camera. SfM is a cost-effective and widely used method for 3D reconstruction that uses a single camera to calculate the photogrammetric properties of objects with respect to the movement of the camera (Xue et al., 2021; Sabato et al., 2017; Qiu et al., 2021; Liu et al., 2020). The principle of the applied approach for SfM can be divided into two main steps: correspondence search and reconstruction, shown in Fig. 3.

The process for SfM starts with capturing multiple images from the arm-mounted RGB camera. Features are computed in each image using descriptors such as Scale-Invariant Feature Transform (SIFT), Speeded-up Robust Features (SURF), or Oriented Fast and Rotated BRIEF (ORB). Then features are matched between sequences of images, and all the outliers are removed using RANSAC. Once a successful match is found with enough inliers, the next step is to verify the geometry of the camera poses. At first, epipolar geometry is calculated, which defines the intrinsic projective geometry between two images which only depends on intrinsic camera parameters. The next step of the process is to find the relationship between two camera poses in the image coordinates. In this step, external camera parameters are used to find the best camera poses to find the homogenous points. This process reconstructs the matched points from two images.

The later stage of SfM relates to the incremental reconstruction of the whole scene shown in Fig. 4 (“Theia Vision Library,” n.d.). The initial step is to initialize the model by using the two-view reconstruction method. Later, the key points of new images are registered with the previous points by estimating the poses and intrinsic camera parameters. Then, previously added key features are assessed using the triangulation method. This triangulation will increase the stability of the model by making it denser. In the end, Bundle Adjustment (BA) refines the reconstructed model by reducing the reprojection error.

3.3. Model fusion by perception enhancement and registration

After the 3D modeling of the target object, the final step is to fuse it with the site surroundings, captured by the RGB-D camera. Fusing both the 3D models present two challenges: scaling and alignment. To solve both problems, affine transformation (point pairs cloud registration method) can be used, transforming the translation, rotation, and scaling between the two coordinate systems.

The affine transformation matrix can store information about translation, rotation, scaling, and shear in a 4×4 matrix. For example,

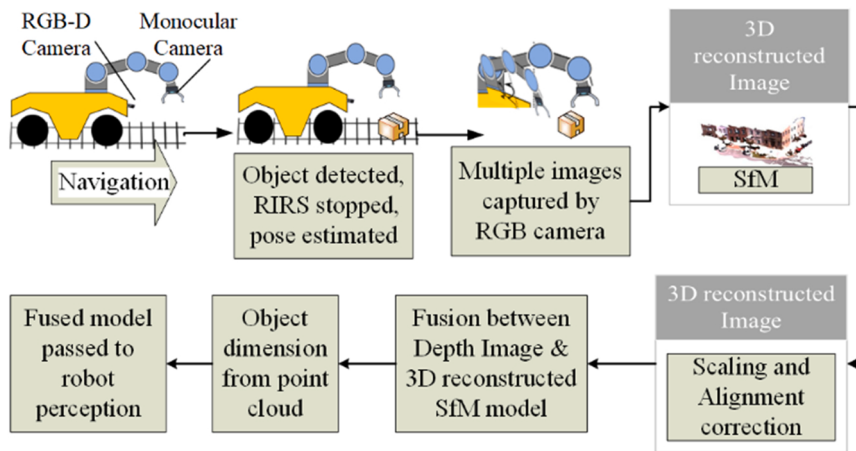


Fig. 2. The architecture of the proposed strategy.

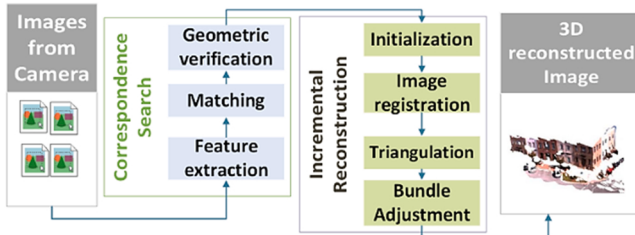


Fig. 3. Workflow of SfM.

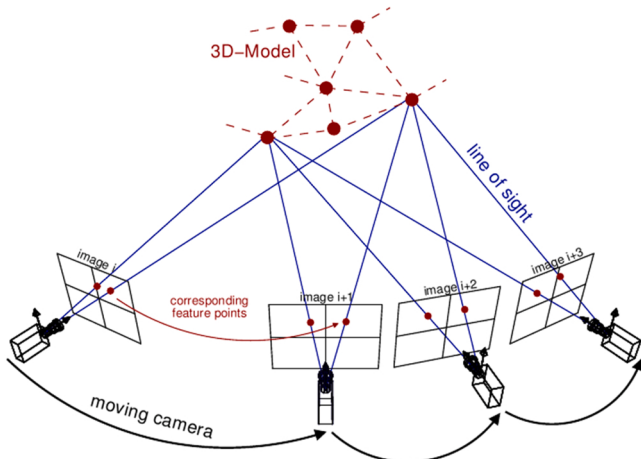


Fig. 4. Reconstruction of 3D points using triangulation ("Theia Vision Library," n.d.).

if there are two points or vectors u and v , the affine transformation matrix M , contains the transformation information between two points or vectors $u(u_x, u_y, u_z)$ and $v(v_x, v_y, v_z)$.

$$u = Mv \quad (1)$$

$$M = \begin{bmatrix} a_{11} & a_{12} & a_{13} & a_{14} \\ a_{21} & a_{22} & a_{23} & a_{24} \\ a_{31} & a_{32} & a_{33} & a_{34} \\ 0 & 0 & 0 & 1 \end{bmatrix} \quad (2)$$

The upper left 3×3 sub-matrix represents rotation, and the right 3×1 sub-matrix represents the translation respectively between two

points. In case there is only translation (points will only move along one or multiple axes), then the translation matrix can be simplified with a translation vector, $t(t_x, t_y, t_z)$.

$$u = \begin{bmatrix} 1 & 0 & 0 & t_x \\ 0 & 1 & 0 & t_y \\ 0 & 0 & 1 & t_z \\ 0 & 0 & 0 & 1 \end{bmatrix} \begin{bmatrix} v_x \\ v_y \\ v_z \\ 1 \end{bmatrix} = \begin{bmatrix} v_x + t_x \\ v_y + t_y \\ v_z + t_z \\ 1 \end{bmatrix} \quad (3)$$

In the case of rotation, three separate 3×3 matrices represent three rotational matrices (R_x, R_y, R_z) along three axes.

Scaling transformation changes the size of the 3D model either by expanding or contracting using a scaling vector, $s(s_x, s_y, s_z)$.

$$u = \begin{bmatrix} s_x & 0 & 0 & 0 \\ 0 & s_y & 0 & 0 \\ 0 & 0 & s_z & 0 \\ 0 & 0 & 0 & 1 \end{bmatrix} \begin{bmatrix} v_x \\ v_y \\ v_z \\ 1 \end{bmatrix} = \begin{bmatrix} s_x v_x \\ s_y v_y \\ s_z v_z \\ 1 \end{bmatrix} \quad (4)$$

Scaling information can be found by measuring the dimensions of a fixed object from the 3D environment created by the RGB-D camera. For the indoor experiment, a wooden pallet was used as the reference object. For the outdoor railway environment, a sleeper or railway track gauge was used as a reference object. For aligning two point clouds, a common object, which is available in both point clouds, can be considered as a reference. Coordinates of 4 points from the reference object will be selected, and that information will be inserted into the corresponding 4 points in the unaligned object to align the 3D model created from SfM.

4. Experiments and results

4.1. Experimental railway system

The experimental system contains two major features: the RIRS and the surrounding environment. An open-source Robot Operating System (ROS) ("ROS Wiki," n.d.) was used to program and control the system. Apart from the open-source benefit, ROS also provides an interactive visualizer called RVIZ, which is useful for real-time data and sensor output visualization ("rviz - ROS Wiki," n.d.). The three cameras have different functionality. The (Pan, Tilt, Zoom) PTZ environment camera can be rotated 360° which is useful to control the RIRS remotely using (Human-Machine Interface) HMI or from a control station. The RIRS and the HMI have been developed as a part of the research initiative from Network Rail, UK, to enable robotic inspection and repair of railway tracks (Demonstration video: Network Rail IN2SMART2, 2022). The Intel Realsense D435i RGB-D camera provides a depth image of the front

environment and can detect an object. The RGB arm camera can be used for close inspection because it is attached to the manipulator, so it can be moved. The RIRS, with all the sensors and the arm, is shown in Fig. 5, while key specifications are given in Table 1.

The experiments have been conducted both in the laboratory, shown in Fig. 6(a), which mimics an off-track scenario, and in a simulated railway test environment, shown in Fig. 6(b), which imitates an on-track scenario. In the laboratory environment, a bottle is used as a target object, while a piece of railway track is used as a target object for the outdoor railway environment. Dimensions of the objects (bottle and rail cut section) and some fixed objects, such as wooden platform and sleeper, are measured manually using a tape measure, and the dimensions are shown in Fig. 7.

Once the Intel Realsense RGB-D camera detects the object, the RIRS will stop. An open-source package called “find object_2d” (Labbé, 2011) is used, which detects the target object based on the pre-defined object library and provides the pose of the object after adding the object in the robot tf. A rosbag (“rosbag - ROS Wiki,” n.d.) has been recorded with depth and tf topic. Later, the “pcl_ros” library was used to convert the bag file to the “.pcd” format point cloud for further processing. Then, 20 images of the object are captured using the RGB camera attached to the manipulator and subsequently processed in VisualSfM (“VisualSfM: A Visual Structure from Motion System,” n.d.) to create the 3D structural reconstruction. VisualSfM is an application for 3D reconstruction that uses multicore processing for faster output (Wu et al., 2011). Finally, both the 3D models were scaled, aligned, and oriented using affine transformation, and the experimental data are available through open access repository (Rahman, Miftahur et al., 2023).

4.2. Results

4.2.1. Object pre-detection by the depth camera

RGB-D camera is mounted on the bulkhead front mount link of the robot and can only visualize the front of the robot. Fig. 8 shows the robot’s perception of the environment from the RGB-D camera. Fig. 8(a) shows the RVIZ visualization for the lab testing scenario (a wood platform, bottle, and nearby environment), and Fig. 8(b) shows the RITA railway track scenario (rails, sleepers, and rail cut section), respectively.

Fig. 9 shows the multiple side views of the 3D model of the bottle and the rail cut section. The front view from the RGB-D camera shows a clear

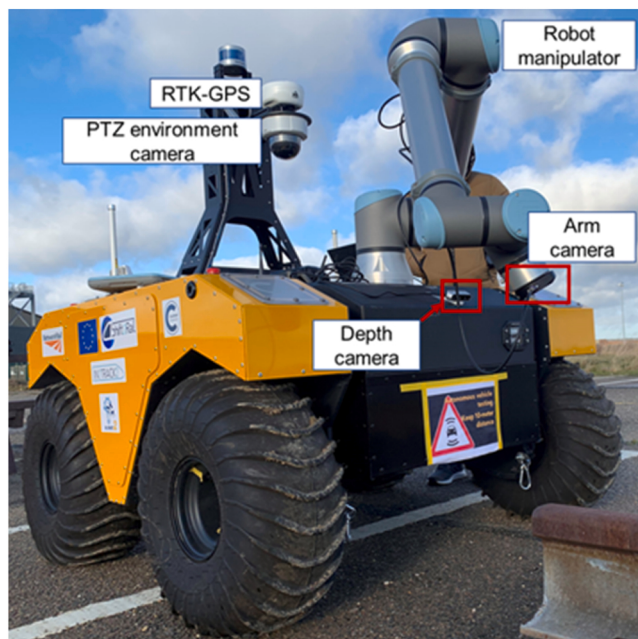


Fig. 5. The RIRS system with the manipulator and sensors.

sense of the target object. However, other sides are not captured. In this point cloud, only the distance from the object to the RIRS platform can be measured. Meanwhile, due to the fixed angle and sensor limitation, there is a slight shape distortion happening at the bottle body and the rail foot in the front view in Fig. 9(a) and (c). Though the RGB-D camera can create a quite dense model of the bottle at the front side, it failed to capture enough point cloud of the rear area, which can be seen in Fig. 9 (b) and (d).

4.2.2. 3D object modeling

In the next step, the SfM technique is used to create a 3D model of the object. RGB camera attached to the manipulator tip has been used to capture 20 images from different perspectives where the objects are fully visible. VisualSfM, an open-source SfM software, was used to create a 3D dense model of the objects for both the indoor lab test and the outdoor railway track test scenarios. A dense 3D reconstructed model of the bottle and rail cut section is shown in Fig. 10.

4.2.3. Model fusion for final perception

Finally, both the 3D model generated from the RGB-D camera and SfM are fused in the CloudCompare software (“CloudCompare,” n.d.). However, the 3D reconstructed models from the SfM do not contain any scaling and alignment information, as shown in Fig. 11. Before fusing both models, and it is important to correct the scaling of the SfM model.

In the railway track test scenario, the dimension of the sleeper between two rails in the British standard gauge is 1435 mm. The distance between two rail feet is 1360 mm, and the width of the sleeper is 224 mm. All of these measurements are constant and are strictly maintained for safety reasons. Using this length and width information, 4 points can be created as a reference coordinate system. Then, these reference points are selected in the 3D reconstructed SfM model to acquire the correct scaling factor. Fig. 13 shows the coordinates of the 4 reference points created for extracting the scaling factor of the 3D reconstructed model. Once the object model is scaled properly, the next step is to fuse the 3D reconstructed model into the RGB-D camera model. During the alignment correction, the point cloud from the RGB-D camera is considered as the fixed model as it contains information about alignment with regard to the robot. Rigid transformation requires at least 3 corresponding points from each model. In this experiment, 4 points are selected from each model for the rigid transformation. Fig. 12 shows the front and side view of the rail cut section after fusion into the RGB-D 3D model.

This experiment diminishes one of the shortcomings of robot perception for railway track inspection and repair work. The RIRS can perform more effectively in track maintenance tasks owing to the better 3D model of the defects and objects created from the fusion between the cameras. Moreover, due to the mobile manipulation capability of the RIRS, this technique can be replicated in many other scenarios apart from rail inspection and repair tasks.

5. Discussion

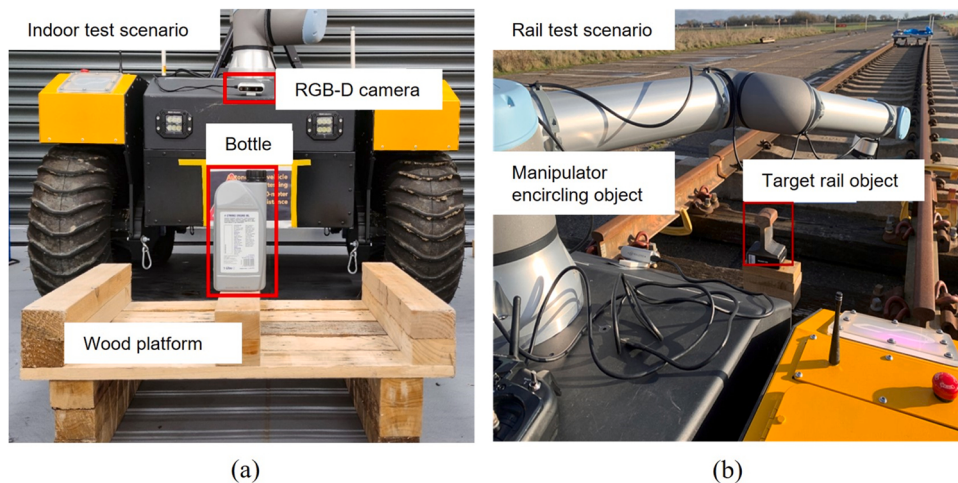
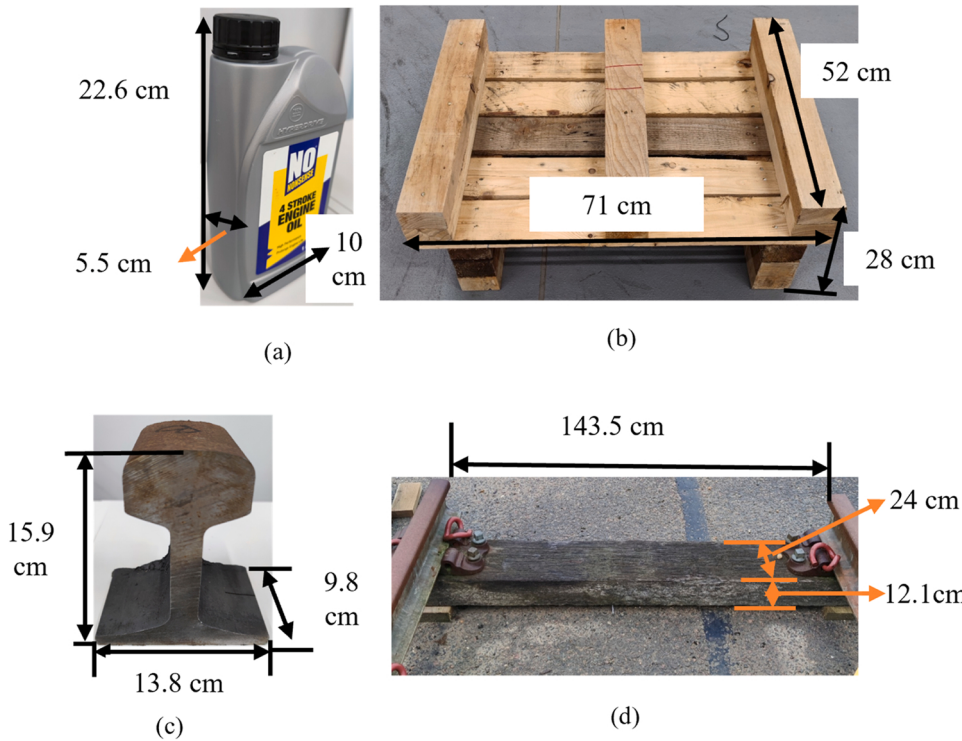
5.1. Image capturing

The 3D model generated from SfM highly depends on the provided images. Two things are very important while capturing and selecting images for SfM; visibility of objects in the image frame and matching between the sequence of images. Images captured for the modeling depend on the manipulator motion trajectory. For this experiment, 20 poses of the manipulator have been pre-set manually to ensure that 100 % of the objects are visible inside the camera frame, as shown in Fig. 14. As the manipulator motion is pre-defined manually without any trajectory planning, the angular difference between each pose is not consistent. It would cause a density inconsistency in the model (Fig. 9 (b) and (d)). Although it has no loss for the object dimension characterization, this density inconsistency may cause some losses on surface

Table 1

Key Specifications of system and sensors in RIRS.

Devices	Brand & models	Mount position	Key specification	Function
Robot arm	UR10e	Base front bulkhead	6 joints, 1300 mm / 51.2 in. of maximum length, 10 kg payload	Creating trajectory
PTZ camera	Axis M5525-E	Sensor tower	Pan range: continuous 360°, Tilt range: 0° to 90°, Optical zoom range: 10, Max video resolution: HDTV 1080p	Environment observation for remote operation
Arm head camera	Robotiq wrist camera	Arm head	Range: 70 mm to infinity; Maximum field of view (cm): 100 * 75 ; Minimum field of view (cm) : 10 * 7.5	Capturing images for 3D reconstruction
RGB-D camera	Intel Realsense D435i	Base front bulkhead	Range: 0.2–20 m, Maximum field of view: Horizontal 870 and vertical 580, Depth Resolution and FPS: 1280 × 720 30fps	Generating perception of the environment

**Fig. 6.** Experimental setup in (a) indoor lab test scenario (b) outdoor RITA railway track test scenario.**Fig. 7.** Dimensions of (a) Indoor target object (bottle), (b) wooden pallet, (c) Outdoor target object (Rail section), and (d) sleepers in a standard gauge railway track.

condition details. Hence, to improve the model density, multiple manipulator trajectory strategies (circular, spherical, and zig-zag concave route, etc.), autonomous trajectory selection, and point cloud

interpolation enhancement are worthy of investigation to provide optimal modeling performance in future research.

Additionally, computation burden and efficiency for model

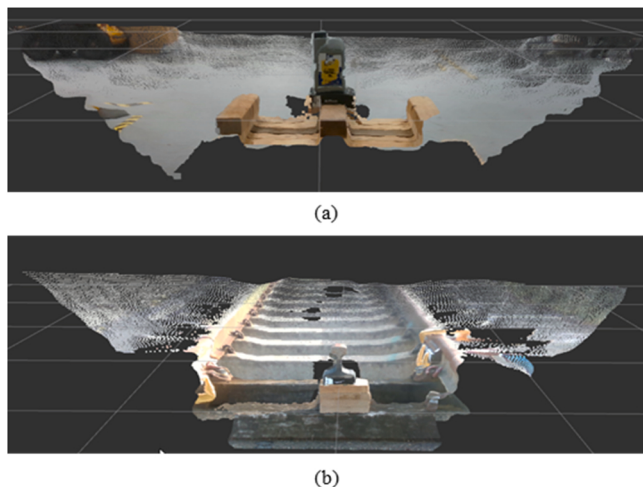


Fig. 8. Perception of the environment from RGB-D camera in (a) indoor lab environment and (b) RITA test area.

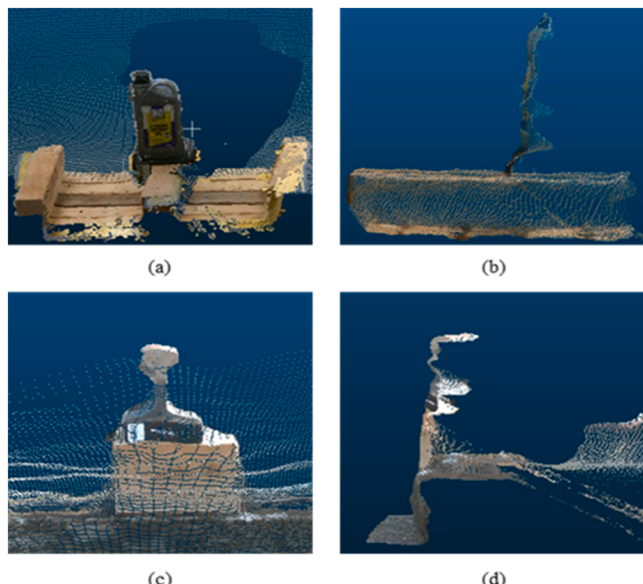


Fig. 9. Front and side view of 3D model of the bottle (a) front, (b) side and rail section (c) front, (d) side captured from an RGB-D camera.

reconstruction follow an increasing trend with the number of images, shown in Fig. 15. In the left case, the reconstruction process took around 1 min when using 20 images. The 3D structure is effectively restored, including the rail head, foot, and web. In another case, it took almost 5 min when 80 images were considered. By consulting with Network Rail railway management engineers, the satisfied the modeling processing duration for one target is suggested to be less than 2 min. In this study, the 20 images case is selected for feasibility validation. For more complex structures or high-resolution images, the optimal balance between quality, efficiency, and computational performance is definitely worth investigating in the future.

5.2. Dimensional accuracy

In the experiments, the scaling factor of the 3D reconstructed model from SfM was corrected using the known dimension of the wood platform and the sleeper. This reconstruction and scaling correction was carried out in 3 repetitions for both the target objects. Then, the mean error for dimensional accuracy was calculated for the scaled 3D model

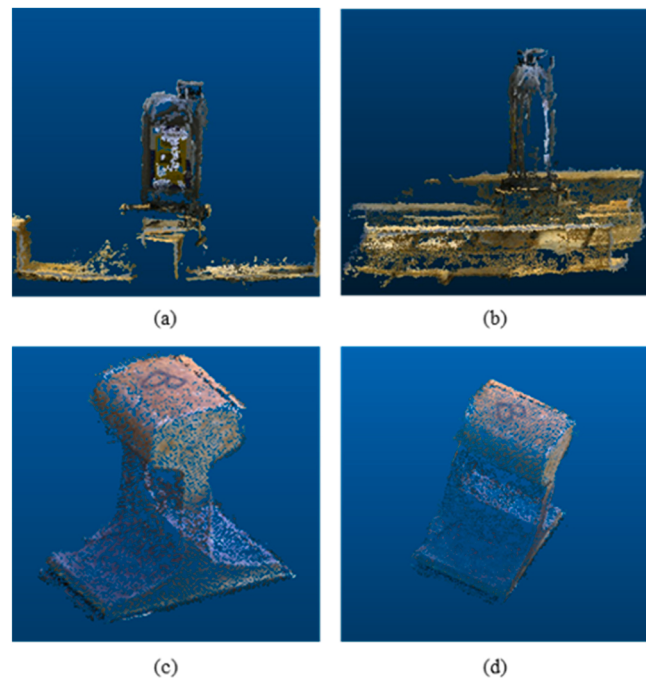


Fig. 10. Dense 3D model of the bottle (a) front view, (b) side view and rail cut section (c) front view, (d) side view is generated by SfM technique using RGB camera and manipulator.

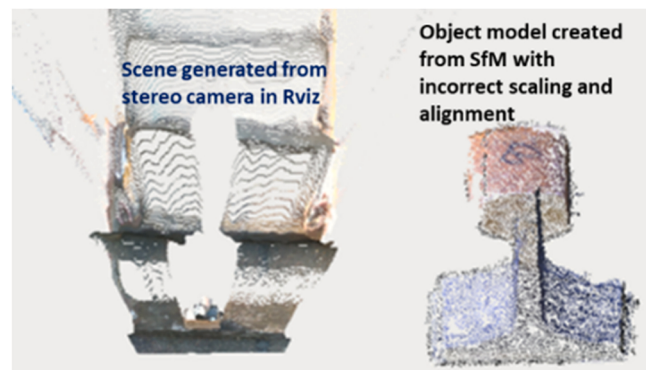


Fig. 11. Wrong scaling and alignment of 3D reconstructed model generated from SfM.

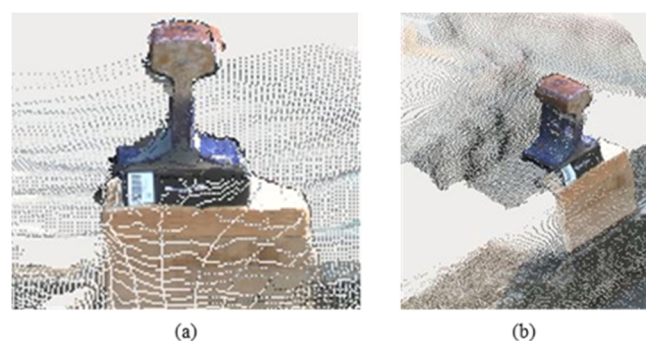


Fig. 12. Fusion of rail model after aligning and scaling (a) front view, (b) side view.

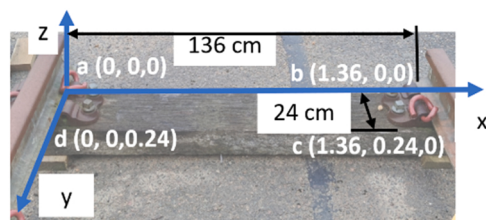


Fig. 13. Reference points created from known dimensions for correcting scaling of SfM model.

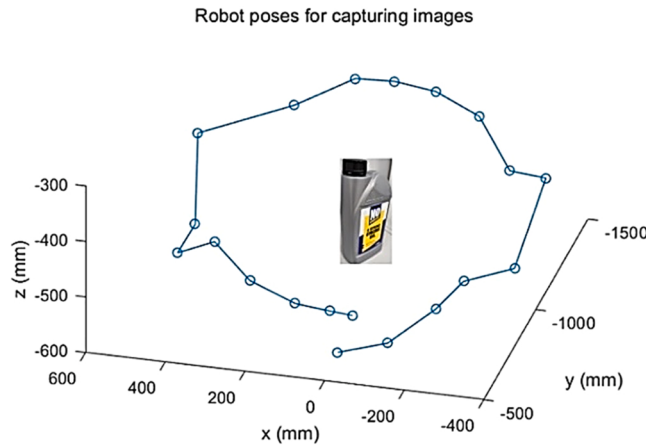


Fig. 14. Manipulator poses for capturing images for data-rich 3D modeling technique.

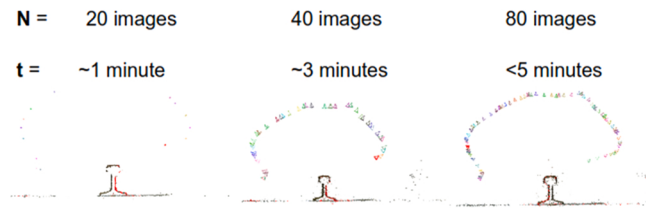


Fig. 15. Test cases for balance between reconstruction time and number of images.

with respect to the actual dimension of the object. The dimensional error observed in Table 2 for the bottle was clearly noticeable at approximately 10.1 %, while the error for the rail cut section is clearly more accurate, with an estimated error of 2.6 %.

The error difference in these 2 objects is attributed to their shape. The bottle has round edges, while the rail section has sharp edges. Sharp edges are important features for SfM to capture and register for creating a 3D model. Another possible reason is that, during the scaling correction process, the chosen 4 reference points are automatically selected

from the background by the point-pair registration method. References are selected from the wooden platform for the laboratory scenario and from the standard British railway track gauge for the track scenario. Low light in indoor and distortion of the wooden platform are the biggest factor for the 4-reference point deviation, which results in the higher dimension error of the bottle modeling in width.

The maximum tolerance of the rail gauge is found to be ± 6 mm which is only 0.41 % of the standard gauge (1435 mm). This tolerance will only affect the scaling factor and around 0.5 % of the model, which is not the main source compared to the mean error value. Additionally, the weight of the rail section can be calculated if required using the 3D measured from the reconstructed model. As per the British railway standard, the weight of a rail section is 60 kg/m for a high-speed railway track. The estimated (mean of repetitions) weight of the modelled rail section is 9.78 kg compared to the ground truth of 9.60 kg.

Currently, the experiments were conducted in a controlled and good lighting condition. It should be noted that lighting conditions such as illumination and reflection will affect the image quality of vision cameras in object detection and modeling. Bad image quality with washed-out color or blur will reduce the accuracy of the reconstructed model. And reflection surface will result in a loss of the surface condition information.

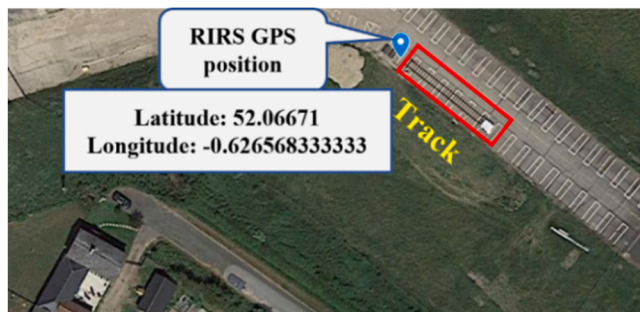
To eliminate the influence, several improvements should be discussed. For the illumination uncertainty, adding an adaptive auxiliary and controlled lighting source on both platform and arm is a good enhancement way to compensate. (Singh et al., 2006; Zhang et al., 2011). For the reflection influence, it is noticed that the reflection issue mainly happens at a certain angle of images within the whole capture trajectory (Ramos et al., 2018). In the future, to compensate for the loss, redundant images captured from different angles around the reflection direction are a promising solution. For instance, at a certain time of the day, the main reflection of the sun on a rail track is predictable. The specific redundant camera poses will help the camera avoid the reflection of the sun influence at a certain time. The system will prepare a group of different trajectories to balance the optimal modeling and lowest reflection.

5.3. Realistic scenario testing

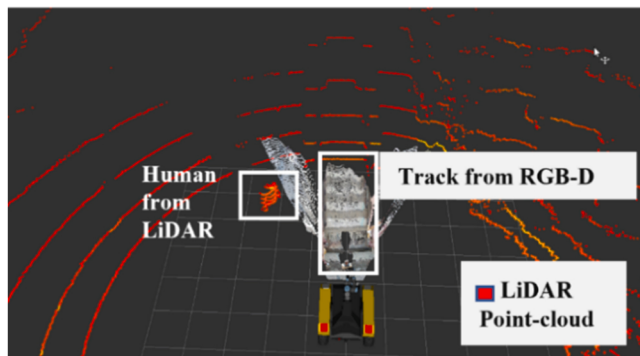
The realistic railway track test proved the feasibility of the proposed method. Fig. 16(a) shows the position of the RIRS in terms of the global map using the GNSS output, which is important to localize the RIRS in the mission control. Fig. 16(b) exhibits two distinct robot perceptions in the form of a depth image from the RGB-D camera and a point cloud of the surrounding environment from LiDAR. Finally, Fig. 16(c) gives an upgraded site-condition model for repair interaction. In this experiment, the tested target object is a pre-set rail section in the middle of the gauge. However, the proposed technique can be easily mirrored to other track components or a foreign obstacle like a fastener, nut, fishplate, etc. The experiment was implemented in the daylight with good illumination, which is paramount to achieving better 3D modeling accuracy. In the future, more arm-fixed illumination lights might be necessary at night. To further improve the impact, the method is to be integrated with Non-

Table 2
Dimensional comparison between actual and 3D reconstructed model.

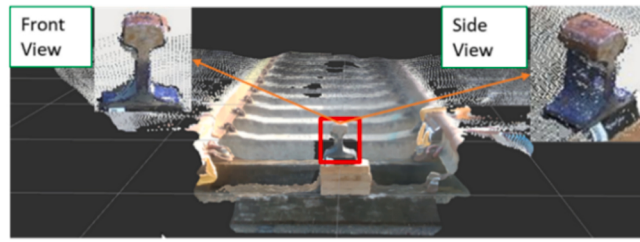
		Bottle		Rail section			
Length	Ground truth (cm)	10.0		10.95	10.83	13.8	14.28
	Reconstructed model (cm)	10.9				14.16	
	Mean Error (%)	9				2.6	
Width	Ground truth (cm)	5.5		5.97	6.06	9.8	10.01
	Reconstructed model (cm)	6.13				9.95	
	Mean Error (%)	10.1				1.7	
Height	Ground truth (cm)	22.6		23.40	23.46	15.9	15.85
	Reconstructed model (cm)	23.32				15.95	
	Mean Error (%)	3.57				0.31	



(a)



(b)



(c)

Fig. 16. Improved RIRS perception with the fused model of maintenance object; (a) RIRS position in global map acquired from GNSS, (b) RIRS perception from RGB-D camera with the surrounding environment from LiDAR, (c) fused 3D model of object in robot perception.

Destructive testing (NDT) results, GNSS geo-location, and the assets survey map to upgrade the infrastructure management database.

5.4. The flexibility of the proposed method

Data-rich high-resolution model of the target environment is one of the desirable features in the digitalization of railway maintenance technology. The proposed technique can not only build the data-rich 3D reconstruction for the maintenance track component but also can be used for railway track survey purposes. In combination with autonomous vehicle control for track travel, this technique can create the 3D reconstruction of the whole track. Fig. 17 presents a pre experiment of modeling along one side of the track around 5.97 m, which includes important track components like fastener clipper, nut & bolt, sleepers, and rail steel. The 3D model well captures the structures and relationships among all components, verifies the feasibility and potential of the proposed technique in track survey or maybe in geometry measurement.

In this trial, we performed the reconstruction implementation with an automated vehicle step forward moving and arm manipulation. The maximum velocity for the vehicle for step forward motion was set to 1 m/s. Each time the robot moves 0.5 m forward and then stops for the manipulator to capture images. This image acquisition process was

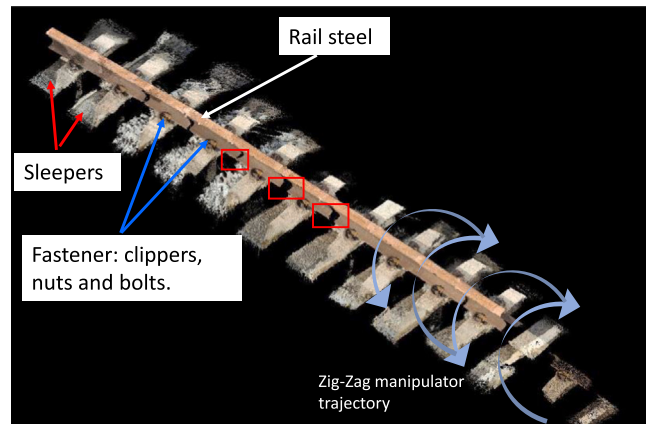


Fig. 17. 3D reconstruction of railway track using SfM with RIRS.

finished in 160 s. It is clear that the orbiting arm trajectory is no longer appropriate for this trial. Therefore, a zig-zag shape trajectory is adopted to ensure the manipulation can cover all components of the track. Once the image-capturing process was finished, the data was transferred to a local computer for post-processing, and a 3D reconstructed model was created using VisualSfM (["VisualSfM: A Visual Structure from Motion System," n.d.](#)). The computer was equipped with intel i7 9700k CPU and RTX 2070 GPU. The reconstruction of the track was completed in less than 6 min.

Most track details are well presented, but there are several missing parts on the side of the rail (red box in Fig. 17.). This is caused by the imperfection of cooperation between vehicle moving and robotic arm manipulation. It can be concluded that the amount of image captured and arm manipulation for 3D reconstruction should be increased and more redundant compared to reconstruction when the vehicle stands still. As the vehicle moves, the blurry motion effect would cause image quality to be lost and registration to be missing while reconstructing. To improve this, the optimal settings of vehicle moving speed and the resolution for arm manipulation sensing will be investigated in the next stage. Nevertheless, this flexibility is a distinctive feature of the proposed technique, which will help to find a solution for the over-massive digital data computation to establish a smart digital infrastructure model.

6. Conclusion

This research proposes a site-condition-based 3D reconstruction technique for railway track components using a robotic sensing system on RIRS. By taking advantage of the sensor fusion of RGB and RGB-D cameras and incorporating the flexibility of a mobile manipulator, a 3D data-rich model of the track component is reconstructed with accurate structural dimension, color, and surface condition. This technique is combined by the autonomous system with robotic sensing to achieve an unmanned, maintenance job-oriented 3D reconstruction for the track.

First, by following the scheduled maintenance job, the RIRS autonomously navigates to the job location. Then from the measuring by a vehicle-based RGB-D camera, the track target component will be focused and pose-estimated to guide a payload mobile manipulator to perform a vision-based 3D reconstruction. Then, the robot manipulator is scheduled a trajectory to automatically reconstruct a dense 3D model using the SfM technique. By orbitally videoing the target, an arm-mounted RGB camera is employed to implement the dense 3D reconstruction with an accurate spatial dimension, volume, color, and surface condition. Finally, the 3D reconstruction is fused with target-surrounding sensing of the vehicle depth camera, 3D Lidar, and geo-location to acquire more digital twin information and the compatibility to fuse with the current infrastructure database.

This research can be utilized as an autonomous digital twin model

generator for the railway maintenance target to support inspection, condition monitoring, and repair task. In addition, a trial of surveying the track along vehicle traveling demonstrates the flexibility and potential of the proposed technique for track survey or maybe geometry measurement. Moreover, the 3D model can provide intuitive visualization and contextualization foundation to support human-involved maintenance tasks if AR systems are combined in future applications. It provides an automation contribution and data-rich enhancement for railway maintenance digital twin and intelligent infrastructure management. To improve the technical performance and address the limitations, the illumination uncertainty, reflection issue, and balance between efficiency and model quality will be focused in the future. The continuous cooperation of optimal manipulator trajectories and traveling vehicle platforms will be investigated to improve the reconstruction execution for a long-track survey and an entire process software will be developed to integrate the control, sensing, and processing to standardize the technique and get rid of commercial software support.

Declaration of Competing Interest

The authors declare the following financial interests/personal relationships which may be considered as potential competing interests. Andrew Starr reports financial support was provided by Network Rail Ltd.

Data Availability

Data will be made available on request.

Acknowledgments

The work was partly supported by the Shift2Rail Joint Undertaking under the European Union's Horizon 2020 research and innovation program under grant agreements No. 881574 and No. 826255. Also, this research is directly supported by Network Rail Limited.

Data supporting this study are openly available from Cranfield Online Research Data at <https://doi.org/10.17862/cranfield.rd.22015574.v1>.

References

- AutoScan – Rail inspection by autonomous systems [WWW Document], n.d. URL <https://cordis.europa.eu/project/id/720506> (accessed 9.25.22).
- Brosque, C., Fischer, M., 2022. Safety, quality, schedule, and cost impacts of ten construction robots. *Constr. Robot* 6, 163–186. <https://doi.org/10.1007/s41693-022-00072-5>.
- Chiaradia, D., Leonardi, D., Manno, V., Solazzi, M., Masini, P., Frisoli, A., 2021. A mobile robot for undercarriage inspection on standard railway tracks. *Mech. Mach. Sci.* 91, 362–369. https://doi.org/10.1007/978-3-030-55807-9_41.
- Chittal, K., Nandhini, M., Krishika, V., Siyo, I.N., Adithyan, J., Gowtham, M., 2017. Autonomous rail inspection, in: 2017 IEEE International Conference on Power, Control, Signals and Instrumentation Engineering (ICPCSI). Presented at the 2017 IEEE International Conference on Power, Control, Signals and Instrumentation Engineering (ICPCSI), pp. 2573–2577. <https://doi.org/10.1109/ICPCSI.2017.8392182>.
- CloudCompare[WWW Document], n.d. URL <https://www.cloudcompare.org/> (accessed 1.18.23).
- da Silva Santos, K.R., de Oliveira, W.R., Villani, E., Dittmann, A., 2023. 3D scanning method for robotised inspection of industrial sealed parts. *Comput. Ind.* 147, 103850. <https://doi.org/10.1016/j.compind.2022.103850>.
- David Jenkins, M., Buggy, T., Morison, G., 2017. An imaging system for visual inspection and structural condition monitoring of railway tunnels, in: 2017 IEEE Workshop on Environmental, Energy, and Structural Monitoring Systems (EESMS). Presented at the 2017 IEEE Workshop on Environmental, Energy, and Structural Monitoring Systems (EESMS), pp. 1–6. <https://doi.org/10.1109/EESMS.2017.8052679>.
- Demonstration video: Network Rail IN2SMART2, 2022. https://www.youtube.com/watch?v=Yh1-pM-txao&ab_channel=profandrewstarr.
- Durazo-Cardenas, I., Starr, A., Turner, C.J., Tiwari, A., Kirkwood, L., Bevilacqua, M., Tsourdos, A., Shehab, E., Baguley, P., Xu, Y., Emmanouilidis, C., 2018. An autonomous system for maintenance scheduling data-rich complex infrastructure: Fusing the railways' condition, planning and cost. *Transp. Res. Part C: Emerg. Technol.* 89, 234–253. <https://doi.org/10.1016/j.trc.2018.02.010>.
- Feng, H., Jiang, Z., Xie, F., Yang, P., Shi, J., Chen, L., 2014. Automatic fastener classification and defect detection in vision-based railway inspection systems. *IEEE Trans. Instrum. Meas.* 63, 877–888. <https://doi.org/10.1109/TIM.2013.2283741>.
- Gibert, X., Patel, V.M., Chellappa, R., 2015. Robust Fastener Detection for Autonomous Visual Railway Track Inspection, in: 2015 IEEE Winter Conference on Applications of Computer Vision. Presented at the 2015 IEEE Winter Conference on Applications of Computer Vision, pp. 694–701. <https://doi.org/10.1109/WACV.2015.98>.
- Giordano, V., 2018. Robotic non-contact rail inspection feasibility study. Cranfield University.
- Great Britain, Treasury, 2020. Treasury Minutes: Government response to the Committee of Public Accounts on the First to the Sixth reports from Session 2019–21.
- Hu, R., Iturralte, K., Linner, T., Zhao, C., Pan, W., Pracucci, A., Bock, T., 2020. A simple framework for the cost–benefit analysis of single-task construction robots based on a case study of a cable-driven facade installation robot. *Buildings* 11, 8. <https://doi.org/10.3390/buildings11010008>.
- IN2SMART2[WWW Document], n.d. URL https://projects.shift2rail.org/s2r_ip3_n.aspx?p=IN2SMART2 (accessed 1.18.23).
- Insa-Iglesias, M., Jenkins, M.D., Morison, G., 2021. 3D visual inspection system framework for structural condition monitoring and analysis. *Autom. Constr.* 128, 103755. <https://doi.org/10.1016/j.autcon.2021.103755>.
- Iyer, S., Velmurugan, T., Gandomi, A.H., Noor Mohammed, V., Saravanan, K., Nandakumar, S., 2021. Structural health monitoring of railway tracks using IoT-based multi-robot system. *Neural Comput. Appl.* 33, 5897–5915. <https://doi.org/10.1007/s00521-020-05366-9>.
- James, J., Wilson, J., Jetto, J., Thomas, A., Dhahabiya, V.K., 2016. Intelligent track cleaning robot, in: 2016 IEEE International Conference on Mechatronics and Automation. Presented at the 2016 IEEE International Conference on Mechatronics and Automation, pp. 332–337. <https://doi.org/10.1109/ICMA.2016.7558584>.
- Kitamura, A., Namekawa, T., Hiramatsu, K., Sankai, Y., 2013. Operating manipulator arm by robot suit HAL for remote in-cell equipment maintenance. *Nucl. Technol.* 184, 310–319. <https://doi.org/10.13182/NT13-A24988>.
- Labbé, M., 2011. Find-Object [WWW Document]. URL <http://introlab.github.io/find-object/> (accessed 7.21.21).
- Li, Q., Ren, S., 2012. A real-time visual inspection system for discrete surface defects of rail heads. *IEEE Trans. Instrum. Meas.* 61, 2189–2199. <https://doi.org/10.1109/TIM.2012.2184959>.
- Liu, S., Acosta-Gamboa, L., Huang, X., Lorence, A., 2017. Novel low cost 3D surface model reconstruction system for plant phenotyping. *J. Imaging* 3, 39. <https://doi.org/10.3390/jimaging3030039>.
- Liu, Y., Qiao, J., Han, T., Li, L., Xu, T., 2020. A 3D image reconstruction model for long tunnel geological estimation. *J. Adv. Transp.* 2020, e8846955. <https://doi.org/10.1155/2020/8846955>.
- Marino, E., Barbieri, L., Colacino, B., Fleri, A.K., Bruno, F., 2021. An augmented reality inspection tool to support workers in Industry 4.0 environments. *Comput. Ind.* 127, 103412. <https://doi.org/10.1016/j.compind.2021.103412>.
- Menendez, E., Victores, J.G., Montero, R., Martínez, S., Balaguer, C., 2018. Tunnel structural inspection and assessment using an autonomous robotic system. *Autom. Constr.* 87, 117–126. <https://doi.org/10.1016/j.autcon.2017.12.001>.
- Our Platform – RailPod, Inc., n.d. URL https://rail-pod.com/?page_id=2527 (accessed 12.25.20).
- Pan, Y.H., Qu, T., Wu, N.Q., Khalgui, M., Huang, G.Q., 2021. Digital twin based real-time production logistics synchronization system in a multi-level computing architecture. *J. Manuf. Syst.*, Digital Twin towards Smart Manufacturing and Industry 4.0 58, 246–260. <https://doi.org/10.1016/j.jmsy.2020.10.015>.
- Panella, F., Roecklinger, N., Vojnovic, L., Loo, Y., Boehm, J., 2020. Cost-benefit analysis of rail tunnel inspection for photogrammetry and laser scanning. *Int. Arch. Photogramm. Remote Sens. Spatial Inf. Sci.* XLIII-B2–2020, 1137–1144. <https://doi.org/10.5194/isprs-archives-XLIII-B2-2020-1137-2020>.
- Pastucha, E., Punia, E., Scislowicz, A., Ćwiakala, P., Niewiem, W., Więcek, P., 2020. 3D reconstruction of power lines using UAV images to monitor corridor clearance. *Remote Sens.* 12, 3698. <https://doi.org/10.3390/rs12223698>.
- Popescu, C., Täljsten, B., Blanksvård, T., Elfgrén, L., 2019. 3D reconstruction of existing concrete bridges using optical methods. *Struct. Infrastruct. Eng.* 15, 912–924. <https://doi.org/10.1080/15732479.2019.1594315>.
- Qiu, W., Jian, L., Cheng, Y., Bai, H., 2021. Three-dimensional reconstruction of tunnel face based on multiple images. *Adv. Civ. Eng.* 2021, e8837309. <https://doi.org/10.1155/2021/8837309>.
- Rahimi, M., Liu, H., Rahman, M., Carcel, C.R., Durazo-Cardenas, I., Starr, A., Hall, A., Anderson, R., 2021. Localisation and Navigation Framework for Autonomous Railway Robotic Inspection and Repair System. Social Science Research Network, Rochester, NY. <https://doi.org/10.2139/ssrn.3945953>.
- Rahman, M., Liu, H., Cardenas, I.D., Starr, A., Hall, A., Anderson, R., 2021a. Towards an Autonomous RIRS: Design, Structure Investigation and Framework, in: 2021 7th International Conference on Mechatronics and Robotics Engineering (ICMRE). Presented at the 2021 7th International Conference on Mechatronics and Robotics Engineering (ICMRE), pp. 164–168. <https://doi.org/10.1109/ICMRE51691.2021.9384846>.
- Rahman, M., Liu, H., Rahimi, M., Carcel, C.R., Kirkwood, L., Durazo-Cardenas, I., Starr, A., 2021b. Investigating Precision and Accuracy of a Robotic Inspection and Repair System (SSRN Scholarly Paper No. ID 3945943). Social Science Research Network, Rochester, NY. <https://doi.org/10.2139/ssrn.3945943>.
- Miftahur Rahman H. Liu M. Masri A. Starr I.D. Cardenas A. Hall R. Anderson Data for a Railway Track Reconstruction Method Using Robotic Vision on a Mobile Manipulator 2023 doi: 10.17862/CRAFIELD.RD.22015574.V1.

- Ramos, P.J., Avendaño, J., Prieto, F.A., 2018. Measurement of the ripening rate on coffee branches by using 3D images in outdoor environments. *Comput. Ind.* 99, 83–95. <https://doi.org/10.1016/j.compind.2018.03.024>.
- Reconstructing Rome [WWW Document], n.d. URL <https://www.computer.org/cSDL/magazine/co/2010/06/mco2010060040/13rRUy3xYe2> (accessed 9.7.21).
- Reyes-Acosta, A.V., Lopez-Juarez, I., Osorio-Companan, R., Lefranc, G., 2019. 3D pipe reconstruction employing video information from mobile robots. *Appl. Soft Comput.* 75, 562–574. <https://doi.org/10.1016/j.asoc.2018.11.016>.
- ROS Wiki [WWW Document], n.d. URL <http://wiki.ros.org/kinetic> (accessed 1.18.23).
- rosbag - ROS Wiki [WWW Document], n.d. URL <http://wiki.ros.org/rosbag> (accessed 1.18.23).
- Rowshandel, H., 2014. *The Development of an Autonomous Robotic Inspection System to Detect and Characterise Rolling Contact Fatigue Cracks in Railway Track (d_ph)*. University of Birmingham.
- rviz - ROS Wiki [WWW Document], n.d. URL <http://wiki.ros.org/rviz> (accessed 1.18.23).
- Sabato, A., Beale, C.H., Nieuzeck, C., 2017. A novel optical investigation technique for railroad track inspection and assessment, in: Nondestructive Characterization and Monitoring of Advanced Materials, Aerospace, and Civil Infrastructure 2017. Presented at the Nondestructive Characterization and Monitoring of Advanced Materials, Aerospace, and Civil Infrastructure 2017, International Society for Optics and Photonics, p. 101692 C. <https://doi.org/10.1117/12.2257831>.
- Singh, M., Singh, S., Jaiswal, J., Hempshall, J., 2006. Autonomous Rail Track Inspection using Vision Based System, in: 2006 IEEE International Conference on Computational Intelligence for Homeland Security and Personal Safety. Presented at the 2006 IEEE International Conference on Computational Intelligence for Homeland Security and Personal Safety, pp. 56–59. <https://doi.org/10.1109/CIHSPS.2006.313313>.
- Stein, D., Spindler, M., Lauer, M., 2016. Model-based rail detection in mobile laser scanning data, in: 2016 IEEE Intelligent Vehicles Symposium (IV). Presented at the 2016 IEEE Intelligent Vehicles Symposium (IV), pp. 654–661. <https://doi.org/10.1109/IVS.2016.7535457>.
- Szeliski, S.A., Yasutaka Furukawa, Noah Snavely, Ian Simon, Brian Curless, Steven M. Seitz, Richard, n.d. Building Rome in a Day [WWW Document]. URL <https://cacm.acm.org/magazines/2011/10/131417-building-rome-in-a-day/fulltext> (accessed 9.7.21).
- Theia Vision Library [WWW Document], n.d. URL <http://www.theia-sfm.org/sfm.html> (accessed 1.18.23).
- Using analytics to get European rail maintenance on track | McKinsey [WWW Document], n.d. URL <https://www.mckinsey.com/industries/public-and-social-sector/our-insights/using-analytics-to-get-european-rail-maintenance-on-track> (accessed 2.7.23).
- VisualSFM : A Visual Structure from Motion System [WWW Document], n.d. URL <http://ccwu.me/vsfm/index.html> (accessed 1.18.23).
- Vithanage, R., Harrison, C., DeSilva, A., 2019. Importance and applications of robotic and autonomous systems (RAS) in railway maintenance sector: a review. *Computers* 8, 56. <https://doi.org/10.3390/computers8030056>.
- Vithanage, R.K.W., Harrison, C.S., Desilva, A.K.M.M., 2019. Enhance 3D Point Cloud Accuracy Through Supervised Machine Learning for Automated Rolling Stock Maintenance: A Railway Sector Case Study. Presented at the Proceedings - 2018 International Conference on Computing, Electronics and Communications Engineering, iCCECE 2018, pp. 242–246. <https://doi.org/10.1109/ICCECOME.2018.8658788>.
- Vithanage, Randika K.W., Harrison, C.S., De Silva, A.K.M., 2019. Autonomous rolling-stock coupler inspection using industrial robots. *Robot. Comput. -Integr. Manuf.* 59, 82–91. <https://doi.org/10.1016/j.rcim.2019.03.009>.
- Wu, C., Agarwal, S., Curless, B., Seitz, S.M., 2011. Multicore bundle adjustment, in: CVPR 2011. Presented at the CVPR 2011, pp. 3057–3064. <https://doi.org/10.1109/CVPR.2011.5995552>.
- Wu, H., Zhu, Q., Guo, Y., Zheng, W., Zhang, L., Wang, Q., Zhou, R., Ding, Y., Wang, W., Pirasteh, S., Liu, M., 2022. Multi-level voxel representations for digital twin models of tunnel geological environment. *Int. J. Appl. Earth Obs. Geoinf.* 112, 102887. <https://doi.org/10.1016/j.jag.2022.102887>.
- Wu, W., Kong, L., Liu, W., Zhang, C., 2018. Laser Sensor Weld Beads Recognition and Reconstruction for Rail Weld Beads Grinding Robot. Presented at the 2017 5th International Conference on Mechanical, Automotive and Materials Engineering, CMAME 2017, pp. 102–105. <https://doi.org/10.1109/CMAME.2017.8540113>.
- Xue, Y., Zhang, S., Zhou, M., Zhu, H., 2021. Novel SFM-DLT method for metro tunnel 3D reconstruction and visualization. *Undergr. Space* 6, 134–141. <https://doi.org/10.1016/j.udsp.2020.01.002>.
- Ye, J., Stewart, E., Roberts, C., 2019. Use of a 3D model to improve the performance of laser-based railway track inspection. *Proceedings of the Institution of Mechanical Engineers, Part F: Journal of Rail and Rapid Transit* 233, 337–355. <https://doi.org/10.1177/0954409718795714>.
- Zhang, Dayi, Jackson, W., Dobie, G., West, G., MacLeod, C., 2022. Structure-from-motion based image unwrapping and stitching for small bore pipe inspections. *Comput. Ind.* 139, 103664. <https://doi.org/10.1016/j.compind.2022.103664>.
- Zhang, Dongyu, Lingamanaik, S.N., Chung, H., 2022. Image-based 3D reconstruction for rail profile measurement. *Proceedings of the Institution of Mechanical Engineers, Part F: Journal of Rail and Rapid Transit* 09544097221110322. <https://doi.org/10.1177/09544097221110322>.
- Zhang, H., Yang, J., Tao, W., Zhao, H., 2011. Vision method of inspecting missing fastening components in high-speed railway. *Appl. Opt., AO* 50, 3658–3665. <https://doi.org/10.1364/AO.50.003658>.
- Zhou, Y., Wang, S., Mei, X., Yin, W., Lin, C., Hu, Q., Mao, Q., 2017. Railway tunnel clearance inspection method based on 3D point cloud from mobile laser scanning. *Sensors* 17, 2055. <https://doi.org/10.3390/s17092055>.
- Zivid, n.d. Zivid Two industrial 3D camera [WWW Document]. URL <https://www.zivid.com/zivid-two> (accessed 2.7.23).
- Zoeteman, A., Esveld, C., 2004. State of the art in railway maintenance management: planning systems and their application in Europe, in: 2004 IEEE International Conference on Systems, Man and Cybernetics (IEEE Cat. No.04CH37583). Presented at the 2004 IEEE International Conference on Systems, Man and Cybernetics (IEEE Cat. No.04CH37583), pp. 4165–4170 vol.5. <https://doi.org/10.1109/ICSMC.2004.1401184>.